JOURNAL OF THERMOPHYSICS AND HEAT TRANSFER
Vol. 13, No. 2, April–June 1999

Influence of Nonequilibrium Kinetics on Heat Transfer and Diffusion near Re-Entering Body

I. Armenise* and M. Capitelli†
University of Bari, 70126 Bari, Italy
and
E. Kustova‡ and E. Nagnibeda§
St. Petersburg University, 198904 St. Petersburg, Russia

The heat transfer and diffusion near the surface of a space vehicle under re-entry conditions are studied on the basis of the kinetic theory of gases. The influence of the nonequilibrium kinetics in an (N_2, N) mixture on the transport properties of the flow is investigated. The nonequilibrium vibrational distributions in the boundary layer near the surface of the re-entering body have been obtained in the state-to-state approach and inserted in the transport kinetic theory code. As a result, the total heat flux, thermal conductivity, and all diffusion coefficients are calculated under different conditions in the freestream and on the surface. The effects of various energy exchanges, vibrational nonequilibrium, dissociation, and recombination on the heat transfer and diffusion are examined.

Nomenclature

c = peculiar velocity
$c_{\mathrm{rot},i}$ = dimensionless rotational specific heat of molecules at the ith vibrational level
c_α = mass fraction of the αth component
D_{T_α} = thermal diffusion coefficients
$D_{\alpha\beta}$ = diffusion coefficients
d_α = diffusion driving force of the αth component
f = stream function
f_{ij} = distribution function
I = unit tensor
i = vibrational quantum number
j = rotational quantum number
k = Boltzmann constant
m = molecular mass
m_a = mass of atoms
n_a = number density of atoms
n_i = number density of a molecule at the ith vibrational level
P = tensor of pressure
Pr = Prandtl number
p = pressure
p_{rel} = relaxation pressure
q = total heat flux
r = spatial coordinate
Sc = Schmidt number
S_i, S_T = source terms
s_j^i = rotational statistical weight
T = gas temperature
t = temporal coordinate
U = total energy per unit mass
u = microscopic molecular velocity
V_a = diffusion velocity of atomic species
V_i = diffusion velocity of molecular species at ith vibrational level
v = macroscopic gas velocity
v_e = flow velocity at the external edge of boundary layer
Z_i^{rot} = rotational partition function
β = velocity gradient along the surface
ε^c = energy of formation of atoms
ε_i = vibrational energy of a molecule
ε_j^i = rotational energy of a molecule at the jth rotational and ith vibrational level
$\langle\varepsilon_j^i\rangle_r$ = averaged rotational energy
ζ = bulk viscosity coefficient
η = body-normal coordinate
θ = dimensionless temperature, T/T_e
λ' = thermal conductivity coefficient
μ = shear viscosity coefficient
ξ = body-parallel coordinate
ρ = density

Subscripts
a = atomic
e = parameters at the external edge of boundary layer
m = molecular
w = parameters at the surface

Introduction

DURING the past several years there has been a growing interest in the investigation of the vibrational and chemical kinetics in different gas flows using the state-to-state approach. This approach becomes particularly important when the characteristic times of vibrational and chemical relaxation are comparable with the macroscopic time of changing of the macroscopic parameters. In this case, the quasistationary distributions over vibrational energy are not valid because of the strong vibrational–chemical coupling that can influence the gas flow parameters. These conditions take place in the expanding flows that are widely cited in the literature (see the brief review in Ref. 1), in the very beginning of the relaxation zone behind a shock wave where the Boltzmann distribution is not established,[2–4] in the conditions of re-entry of the space vehicles into planetary atmospheres,[5] and in the end-wall boundary layer behind a shock wave in a shock tube.[6] In Refs.

Received March 2, 1998; revision received Oct. 15, 1998; accepted for publication Oct. 23, 1998.

*Researcher, Chemistry Department, Centro di Studio per la Chimica dei Plasmi del CNR, Via Orabona 4.
†Professor, Chemistry Department, Centro di Studio per la Chimica dei Plasmi del CNR, Via Orabona 4.
‡Assistant Professor, Mathematics and Mechanics Department, Bibliotechnaya pl. 2.
§Professor, Mathematics and Mechanics Department, Bibliotechnaya pl. 2.

5 and 7, it is shown that strong nonequilibrium conditions exist near the surface of the spacecraft entering the air atmosphere with the hypersonic speed. The non-Boltzmann distributions appear as a result of the gas temperature decrease from the high shock-edge value toward the temperature of the cool vehicle surface. In the result, the vibrational temperature in the boundary layer occurs higher, compared with the gas temperature and the interplay of the vibrational energy exchanges; dissociation and recombination may dramatically change the vibrational level populations. The essentially non-Boltzmann behavior of the vibrational populations in the stagnation zone near a blunt body was shown also in Ref. 8.

Near the surface of the spacecraft, the dissipative processes of heat transfer and diffusion are of importance and should be considered together with the vibrational–chemical kinetics. Usually the nonequilibrium processes in the boundary layer are studied using either the weak nonequilibrium and two-temperature kinetic theory approaches[9–11] or the framework of the phenomenological models. The state-to-state approach to this problem has not been sufficiently advanced up to now, and few results have been obtained using the simple empirical models for transport coefficients.[8,12]

The present paper studies the effect of nonequilibrium distributions on the transport properties near a re-entering body on the basis of the state-to-state kinetic theory developed in Refs. 2 and 13. The detailed kinetics in the boundary layer, investigated on the basis of the model,[5] is inserted in the kinetic theory code.[13] As a result, the heat flux, thermal conductivity, and all diffusion coefficients are calculated in the (N_2, N) mixture, with dissociation and recombination under different conditions in the freestream and at the vehicle surface.

Equations of State-to-State Kinetics in the Gas Flow: Transport Properties

We consider a binary mixture of dissociating diatomic molecules and atoms under the conditions of rapid equilibration of translation and rotational energies compared with vibrational relaxation and dissociation–recombination processes. The characteristic times of slow processes are of the same order as the macroscopic time. In this case, the following system of the equations of the detailed vibrational and chemical kinetics in a gas flow coupled with the momentum and energy conservation equations is obtained from the kinetic equations for the distribution functions[13]:

$$\frac{dn_i}{dt} + n_i\nabla\cdot v + \nabla\cdot(n_iV_i) = R_i, \qquad i = 0, 1, \ldots \tag{1}$$

$$\frac{dn_a}{dt} + n_a\,\nabla\cdot v + \nabla\cdot(n_aV_a) = R_a \tag{2}$$

$$\rho\frac{dv}{dt} + \nabla\cdot P = 0 \tag{3}$$

$$\rho\frac{dU}{dt} + \nabla\cdot q + P\colon\nabla v = 0 \tag{4}$$

Equations (1) and (2) contain the diffusion velocities for each vibrational level V_i and atomic species V_a. The right-hand sides of Eqs. (1) and (2) describe the change of molecular level populations and atomic densities caused by the vibrational energy exchanges, dissociation, and recombination:

$$R_i = R_i^{\text{vibr}} + R_i^{\text{diss-rec}}, \qquad R_a = -2\sum_i R_i^{\text{diss-rec}} \tag{5}$$

The source terms R_i^{vibr} and $R_i^{\text{diss-rec}}$ contain the microscopic rate constants of the corresponding processes that are expressed in terms of the inelastic collision integrals.

Hereafter, we follow the code of the transport kinetic theory in the level approach developed in Refs. 2 and 13, and use the algorithm of the calculation of the transport terms in Eqs. (1–4) given in these papers.

Transport and production terms in Eqs. (1–4) are defined by the distribution functions. Using the generalized Chapman–Enskog method in the state-to-state approach, the distribution functions in each approximation are expressed in terms of the functions $n_i(r, t)$, $n_a(r, t)$, $v(r, t)$, and $T(r, t)$. The zero-order distribution functions for molecules at the ith vibrational and jth rotational level $f_{ij}^{(0)}$ and atoms $f_a^{(0)}$ are given by

$$f_{ij}^{(0)} = \left(\frac{m}{2\pi kT}\right)^{3/2} s_j^i\,\frac{n_i}{Z_i^{\text{rot}}(T)}\exp\left(-\frac{mc^2}{2kT} - \frac{\varepsilon_j^i}{kT}\right)$$
$$f_a^{(0)} = \left(\frac{m_a}{2\pi kT}\right)^{3/2} n_a\exp\left(-\frac{m_ac_a^2}{2kT}\right) \tag{6}$$

In the zero-order approximation, because of the Maxwell distribution over velocities, the heat flux and diffusion velocities are equal to zero, and the pressure tensor $P^{(0)} = pI$. In this case, Eqs. (1–4) describe the flow of a mixture of nonviscous nonconductive gases. Usually this approach is used for the modeling of the vibrational–chemical kinetics behind shock waves and in expanding flows, neglecting the influence of the transport processes on the vibrational and chemical kinetics. Near the surface of the space vehicle, the non-Maxwellian velocity distribution should be taken into account, and heat transfer and diffusion processes should be considered together with the nonequilibrium kinetics.

In the first-order approximation the pressure tensor has the form

$$P = (p - p_{\text{rel}})I - 2\mu S - \zeta\nabla\cdot vI \tag{7}$$

The diffusion velocities are defined by the following expressions[13]:

$$V_i = -D_{ii}d_i - D_{mm}\sum_{k\neq i} d_k - D_{ma}d_a - D_{T_m}\nabla\,\ell n\,T \tag{8}$$

$$V_a = -D_{aa}d_a - D_{ma}d_m - D_{T_a}\nabla\,\ell n\,T \tag{9}$$

where the diffusion driving forces for molecules at different vibrational levels and atoms are given by

$$d_i = \nabla\left(\frac{n_i}{n}\right) + \left(\frac{n_i}{n} - \frac{\rho_i}{\rho}\right)\nabla\,\ell n\,p$$
$$d_a = \nabla\left(\frac{n_a}{n}\right) + \left(\frac{n_a}{n} - \frac{\rho_a}{\rho}\right)\nabla\,\ell n\,p \tag{10}$$

Equations (8) and (9) contain the following diffusion coefficients: D_{T_m} and D_{T_a} are the thermal diffusion coefficients of molecules and atoms correspondingly, D_{ma} is the diffusion coefficient for a mixture of molecules and atoms, D_{mm} is the diffusion coefficient of the molecules at different vibrational levels, D_{aa} is the self-diffusion coefficient of atomic species, and D_{ii} are the self-diffusion coefficients of the molecular species at the same ith vibrational level. $n = \Sigma_i\, n_i + n_a$, $\rho_i = mn_i$, $\rho_a = m_an_a$, $\rho = \Sigma_i\,\rho_i + \rho_a$.

The total heat flux in the state-to-state approach has the next form:

$$q = -\lambda'\nabla T - p(D_{T_m}d_m + D_{T_a}d_a)$$
$$+ \sum_i\left(\frac{5}{2}kT + \langle\varepsilon_j^i\rangle_r + \varepsilon_i\right)n_iV_i + \left(\frac{5}{2}kT + \varepsilon^a\right)n_aV_a \tag{11}$$

The total heat conductivity coefficient λ' is a sum of two coefficients λ'_r and λ'_r, describing the transport of translational and rotational energy correspondingly.

One can see that the diffusion velocities and heat flux in the level approach are defined not only by the gradients of the gas temperature and number densities of atomic and molecular species, but also by the gradients of all vibrational level populations.

The algorithm of the calculation of the thermal conductivity and all diffusion coefficients is developed in Ref. 13. In the first-order approximation of the generalized Chapman–Enskog method, the following formulas are obtained:

$$\lambda' = \sum_i \frac{5}{4} k \frac{n_i}{n} a_{mi,10} + \frac{5}{4} k \frac{n_a}{n} a_{ai,10} + \sum_i \frac{k}{2} \frac{n_i}{n} c_{\mathrm{rot},i} a_{mi,01} \quad (12)$$

$$D_{ma} = \frac{1}{2n} d^a_{m,0}, \quad D_{mm} = \frac{1}{2n} d^m_{m,0}, \quad D_{aa} = \frac{1}{2n} d^a_{a,0}, \quad D_{ii} = \frac{1}{2n} d^i_{i,0} \quad (13)$$

$$D_{T_a} = -\frac{1}{2n} a_{ai,00}, \qquad D_{T_m} = -\frac{1}{2n} a_{mi,00} \quad (14)$$

Here, the coefficients $a_{\alpha i,00}$, $a_{\alpha i,01}$, $a_{\alpha i,10}$ ($\alpha = m, a$), $d^\beta_{\alpha,0}$ ($\alpha, \beta = m, a, i$) are the solutions of the linear algebraic equations, and can be found as a ratio of the determinants. The elements of the determinants depend on the elastic collision integrals, vibrational level populations, atomic number densities, and gas temperature.

The expressions for q and V_i, V_a differ from those obtained in the one-temperature approach[14–16] and in the case of weak deviations from the equilibrium.[17] In the first case, they contain the gradients of the gas temperature and number densities of atoms and molecules, which are found as a solution of the equations of the one-temperature chemical kinetics based on the Boltzmann distribution over vibrational levels with the gas temperature. In the latter case, the number densities of chemical species can be found from the equations of the thermodynamic equilibrium.

Equations (1–4), with transport terms (7–9) and (11) and transport coefficients (12–14), describe the simultaneous processes of the nonequilibrium kinetics and heat transfer and diffusion in the flow. The development of the two- and three-dimensional numerical codes for these equations is rather difficult because of the large number of differential equations for the level populations and high number of the diffusion coefficients for the various vibrational levels of molecular species. In fact, the calculation of all transport coefficients in the state-to-state approach requires the computation of the determinants containing a large number of elements in multicomponent reacting mixtures.[13] The one-dimensional code is useful for the understanding of the kinetics in flows such as that behind a shock wave, in a nozzle and expanding tube, and in a nonequilibrium boundary layer. In the present paper, the one-dimensional approximation developed in Ref. 5 for the flow in a boundary layer near the surface is used. Moreover, the following simplification of the problem is suggested as the first step toward the final goal of the solution of the full system of Eqs. (1–4), (7–9), (11), and (12–14) for multicomponent reacting mixtures. First, the nonequilibrium vibrational level populations, gas temperature, and number density of atomic species are found from the equations that may be obtained from Eqs. (1–4), after some simplification of the transport terms. This model is described in the next section. Then, having this solution, the rigorous kinetic transport theory code given in the preceding text is used for the simulation of the transport properties, such as heat transfer and diffusion in the same flow. This approach permits us to calculate the heat conductivity and all diffusion coefficients as well as the total heat flux, taking into account the strong nonequilibrium distributions, and to estimate the influence of the nonequilibrium kinetics on the transport properties near the surface of a space vehicle.

Nonequilibrium Kinetics in a Boundary Layer

The calculation of the level populations, number densities of atoms, and gas temperature in a boundary layer near the surface of the spacecraft was performed using the approximate code developed in Refs. 5, 7, and 18. In these papers, the equations of the state-to-state kinetics and fluid dynamics were simplified for the case of a stationary flow near a flat plate in the stagnation point approximation. The model allows the computation of the vibrational distributions, the atomic density, and the gas temperature profiles along a coordinate normal to the surface.

For a binary mixture (N_2, N), the one-dimensional equations of the fluid dynamics and state-to-state kinetics in the boundary layer have been solved:

$$c_i'' + Scfc_i' = S_i, \qquad i = 0–46 \quad (15)$$

$$\theta'' + Prf\theta' = S_T \quad (16)$$

Here, Eqs. (15) are the equations for the populations of the bounded vibrational levels $c_i = \rho_i/\rho$ ($i = 0–45$) and atoms $c_{46} = c_a = \rho_a/\rho$ ($i = 46$). Equation (16) is the energy equation. The derivatives have been derived with respect to coordinate η normal to the surface:

$$\eta = \frac{\nu_e}{\sqrt{2\xi}} \int_0^y \rho \, dy, \qquad \xi = \int_0^x \rho_e \nu_e \, dx$$

In Eqs. (15) and (16) the left-hand side corresponds to the diffusive and convection terms. The Schmidt and Prandtl numbers are assumed to be constant. The source terms S_i and S_T rise from the vibrational–vibrational (VV) and vibrational–translational (VT) energy exchange, as well as from the dissociation–recombination processes.[5,18] The vibrational kinetics in nitrogen includes the following processes:

$$N_2(i) + N_2(w) \leftrightarrow N_2(i-1) + N_2(w+1) \quad (17)$$

$$N_2(i) + N_2 \leftrightarrow N_2(i-1) + N_2 \quad (18)$$

$$N_2(i) + N \leftrightarrow N_2(w) + N \quad (19)$$

The rate coefficients of processes (17–19) have been taken from Refs. 12, 19, and 20, respectively. Concerning dissociation–recombination reactions, the ladder-climbing model is used. We consider a pseudolevel $i' + 1$ located just above the last bounded level of a molecule i', through which the dissociation–recombination reaction passes:

$$N_2(i) + N_2(i') \leftrightarrow N_2(i-1) + N_2(i'+1) \leftrightarrow N_2(i-1) + 2N \quad (20)$$

$$N_2(i') + N_2 \leftrightarrow N_2(i'+1) + N_2 \leftrightarrow 2N + N_2 \quad (21)$$

$$N_2(i) + N \leftrightarrow N_2(i'+1) + N \leftrightarrow 3N \quad (22)$$

The dissociation rates have been calculated as an extension to the pseudolevel of the VV- and VT-exchange rates, whereas the recombination rates are obtained using the detailed balance principle.[5,7]

The following boundary conditions for Eqs. (15) and (16) are considered. At the external edge of the boundary layer, the temperature, density, and pressure are fixed: $T = T_e$, $\rho = \rho_e$, $p = p_e$; the vibrational distributions are assumed to be the Boltzmann equilibrium at the gas temperature $c_i = c_i^{(eq)}(T_e)$. The

surface temperature is also fixed: $T = T_w$; the surface is considered as noncatalytic: $(\partial c_i/\partial\eta)_w = 0$. The velocity gradient along the surface $\beta = dv_e/dx$ is the parameter fixed at 5000 s^{-1}; β can be treated as the inverse of the residence time of a particle in the boundary layer.

This approximation allows one to calculate the vibrational level populations, atomic population density, temperature, and temperature gradient along the coordinate η.

These results have been inserted into the kinetic theory code described in the previous section. In the boundary-layer approximation, the pressure gradient is equal to zero and expressions (10) for the diffusion driving forces may be simplified. The diffusion velocities [Eqs. (8) and (9)] take the form

$$V_i = -(D_{ii} - D_{mm})\nabla\left(\frac{n_i}{n}\right) - D_{mm}\nabla\left(\frac{n_m}{n}\right) - D_{ma}\nabla\left(\frac{n_a}{n}\right) - D_{T_m}\nabla \ell n\, T \tag{23}$$

$$V_a = -D_{aa}\nabla\left(\frac{n_a}{n}\right) - D_{ma}\nabla\left(\frac{n_m}{n}\right) - D_{T_a}\nabla \ell n\, T \tag{24}$$

Finally, the heat conductivity and all diffusion coefficients, and the total energy flux and its Fourier part, depending only on the gas temperature gradient, have been calculated for the same conditions along the coordinate η. The results show the influence of the nonequilibrium kinetics on the transport processes in the flow, and they are discussed in the next section.

Results and Discussion

Using the models of the transport properties and nonequilibrium kinetics presented in the previous sections, we investigated the vibrational and dissociation–recombination kinetics and heat transfer and diffusion in the flow of an (N_2, N) mixture in the boundary layer under re-entry conditions: high temperature at the edge of the boundary layer ($\eta = 4$): $T_e = 5000$ and 7000 K, and low temperature of the vehicle surface ($\eta = 0$): $T_w = 300$ and 1000 K. The second case ($T_e = 7000$ and 1000 K) approximately corresponds to the Mach number in the freestream, ~25. Two values of the pressure outside the boundary layer are considered: $p_e = 10^3$ and 10^6 Pa. Also, two different models are examined. The first one includes the complete kinetics described in the previous section: VT and VV exchange, recombination, and dissociation; and in the second model recombination and VV exchanges are neglected. The comparison of the vibrational distributions, macroscopic parameters, and transport properties of the flow in both cases permits one to estimate the effects of recombination and VV exchange.

First we will discuss the results concerning the nonequilibrium kinetics in the conditions under consideration. Figures 1a and 1b represent the dimensionless level populations n_i/n of N_2 vs i at the different distances from the wall ($p_e = 10^3$ Pa). Dissociation in the gas flow near the high-temperature edge of the boundary layer produces nitrogen atoms that diffuse toward the cool surface. Recombination near the surface pumps the populations of the upper levels. As a result of this process, and VV and VT exchange, the strong nonequilibrium distribution with the plateau section at the intermediate and upper levels appears near the wall (see Fig. 1a). This effect was found in Refs. 5, 7, and 18. The role of recombination and VV exchange can be seen from the comparison of Figs. 1a and 1b, where the level populations are given for the case when recombination and VV exchange were neglected. Figure 1b shows the deactivation of the vibrational levels from the edge of the boundary layer toward the surface, the distributions are not far from the steady-state ones.

Figures 2a and 2b report the level populations vs i and the profiles of the populations of the selected levels ($i = 0$, $i = 10$, $i = 20$, $i = 45$) in the case of $p_e = 10^6$ Pa. In this case, the relaxation times of all processes are shorter as a result of the high pressure, and the difference between level populations at various p_e is evident. In particular, at higher pressures, the region near the surface where the strong nonequilibrium distributions are observed is more narrow, and the populations of the intermediate levels near the wall are lower. From Fig. 2b,

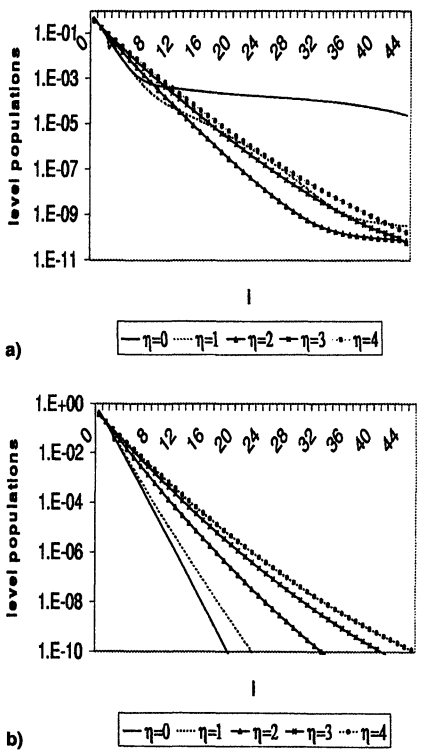

Fig. 1 Reduced level populations, n_i/n, as functions of i at different η (T_e = 5000 K, T_w = 300 K, $p_e = 10^3$ Pa): a) complete kinetics and b) no VV exchange and recombination.

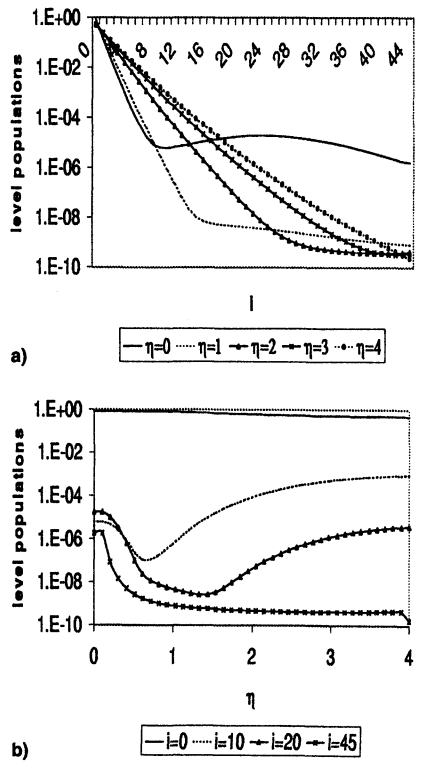

Fig. 2 Reduced level populations a) n_i/n, as functions of i at different η (T_e = 5000 K, T_w = 300 K, $p_e = 10^6$ Pa). b) Populations of selected levels as functions of η.

the maximum gradients of the nonequilibrium level populations are seen in the region $0 < \eta < 2$.

Figure 3 gives the change of the number density of the N atoms in the boundary layer at different conditions. The strong dependence of n_N on the pressure p_e is found: under the high-pressure conditions, the concentration of atoms is much lower because of the low degree of dissociation. One can see also that, in the $p_e = 10^3$ Pa case, the influence of recombination and VV exchange on the number density of species is important in the interval $0 < \eta < 2$, where the vibrational distributions deviate more strongly from the equilibrium. It may be noticed that the influence of recombination on n_N is much less than on n_i. It is not surprising and may be explained by two reasons: first, the surface is noncatalytic, and second, according to the ladder-climbing model, dissociation and recombination go through one vibrational pseudolevel $i' + 1$ and do not significantly change the total number density of species.

The temperature profile is given in Fig. 4 for the same conditions. The temperature gradient has also been calculated. The temperature decreases and the temperature gradient increases from the edge toward the surface (with η decrease). Recombination near the surface leads to an increase in $dT/d\eta$ at $\eta < 0.6$. In the case of high pressure, $p_e = 10^6$ Pa $dT/d\eta$ near the wall is less than in the $p_e = 10^3$ Pa case at $0 < \eta < 2$, and exceeds $dT/d\eta$ calculated at a low pressure at $\eta > 2$. It is because of the fact that in this case the dissociation near the edge of the boundary layer and recombination near the wall are compensated by the corresponding reverse process.

Now we will consider the effect of the nonequilibrium kinetics on the heat conductivity and diffusion coefficients and the total heat flux in the boundary layer. In Fig. 5 the heat conductivity coefficient vs η is plotted. It is seen that λ' increases with the temperature (toward the edge of the boundary layer). Changing the vibrational distributions only slightly affects the thermal conductivity coefficient. Actually, neglect of recombination and VV exchange gives an underestimation of λ' ~5–8% at $\eta < 1$; this discrepancy disappears with rising η. Increasing the pressure p_e leads to a decrease of λ' ~5–12%. In a nondissociating gas, λ' is known to increase with pressure. The decrease of λ' with p_e rising in a dissociating gas may be seen from experimental data,[21] and can be explained by the fact that, at $p_e = 10^6$ Pa, the molar fraction of atoms in the flow is less than the one at $p = 10^3$ Pa, and it leads to a decrease of the total translational energy of the unit of mass. Because the contribution of the translational energy to the total heat conductivity coefficient exceeds the contribution of the rotational degrees of freedom,[11,22] the decrease in the translational energy storage is not compensated by the corresponding increase in the rotational energy stock because of the rise of the molecular molar fraction. Therefore, λ' describing the transport of translational and rotational energy decreases with pressure.

The results of the calculation of the diffusion coefficients are given in Figs. 6–8. Figure 6 presents the diffusion and self-diffusion coefficients D_{N_2-N}, $D_{N_2-N_2}$, $(i \neq k)$, D_{N-N}, depending on η at $p_e = 10^3$ Pa. It is seen that the D_{N-N} coefficient exceeds two other diffusion coefficients. The behavior of the thermal diffusion coefficients is similar; they increase with η but are about an order of magnitude less compared with the other diffusion coefficients. In the approximate calculation of the heat flux, the terms containing the thermal diffusion coefficients are often neglected.[8,15] However, under the strong nonequilibrium conditions, when the gradients of the macroscopic parameters are high, the thermal diffusion process may give a significant contribution to the total energy transfer.

The self-diffusion coefficients for each vibrational level D_{ii} are given in Figs. 7a and 7b as functions of i for different

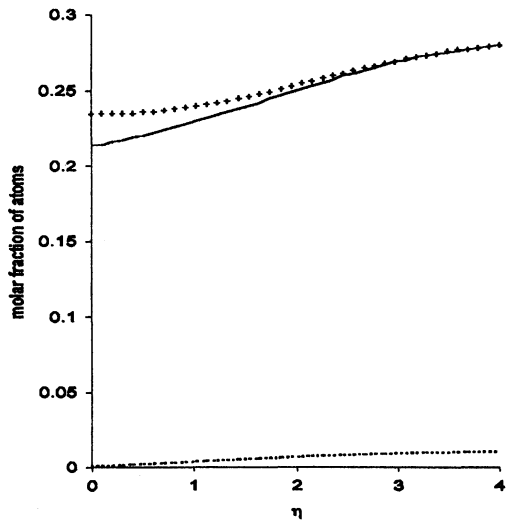

Fig. 3 Molar fraction of atoms as a function of η. $T_e = 5000$ K and $T_w = 300$ K. Solid curve, $p_e = 10^3$ Pa, complete kinetics; points, $p_e = 10^3$ Pa, no VV exchange and recombination; dotted curve, $p_e = 10^6$ Pa.

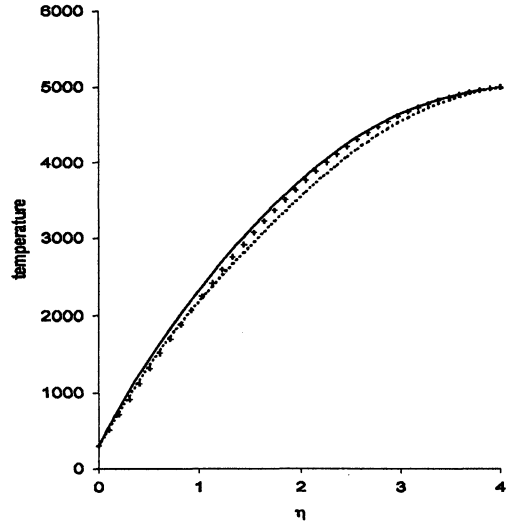

Fig. 4 Gas temperature T, in K, as a function of η. $T_e = 5000$ K and $T_w = 300$ K. Solid curve, $p_e = 10^3$ Pa, complete kinetics; points, $p_e = 10^3$ Pa, no VV exchange and recombination; dotted curve, $p_e = 10^6$ Pa.

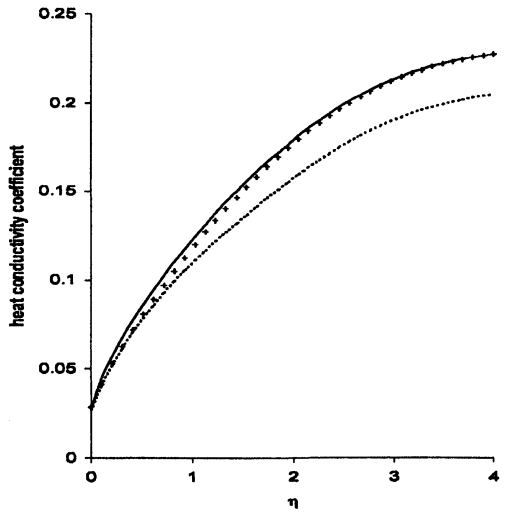

Fig. 5 Heat conductivity coefficient λ', in W/m K, as a function of η. $T_e = 5000$ K and $T_w = 300$ K. Solid curve, $p_e = 10^3$ Pa, complete kinetics; points, $p_e = 10^3$ Pa, VV exchange and recombination are neglected; dotted curve, $p_e = 10^6$ Pa.

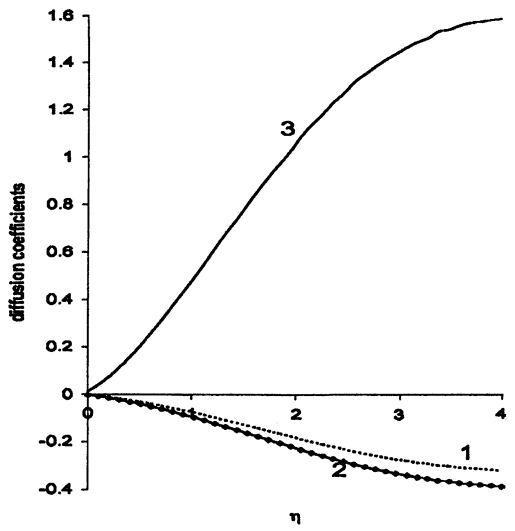

Fig. 6 Diffusion coefficients D_{ij}, in m²/s, as functions of η. T_e = 5000 K, T_w = 300 K, and $p_e = 10^3$ Pa. Curves 1, D_{N_2-N}; curves 2, $D_{N_2-N_2}$ ($i \neq k$); curve 3, D_{N-N}.

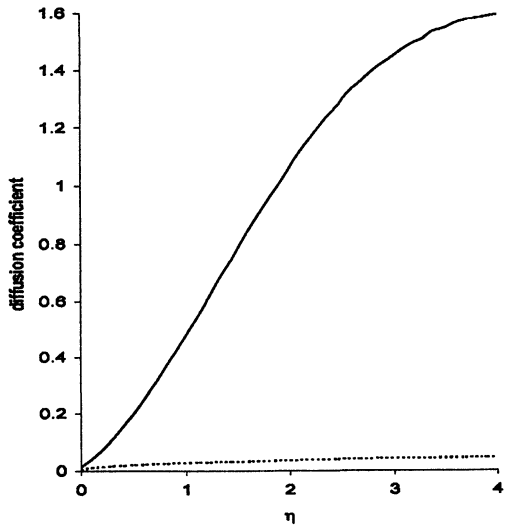

Fig. 8 Diffusion coefficient D_{N-N}, in m²/s, as a function of η. T_e = 5000 K and T_w = 300 K. Solid curve, $p_e = 10^3$ Pa; dotted line, $p_e = 10^6$ Pa.

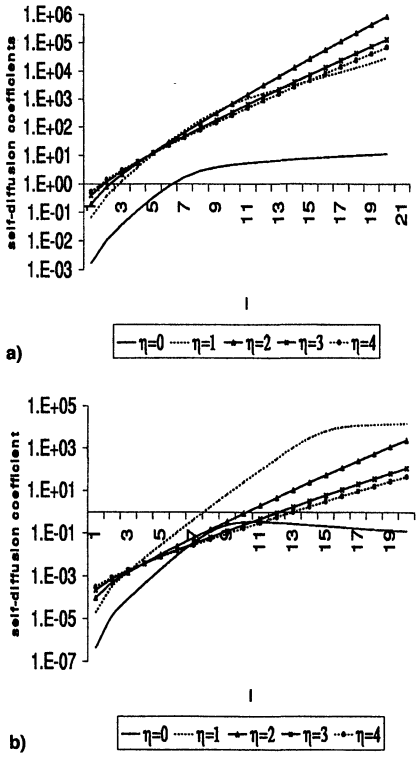

Fig. 7 Self-diffusion coefficients D_{ii}, in m²/s, as a function of i at different η. T_e = 5000 K, T_w = 300 K. p_e = a) 10^3 and b) 10^6 Pa.

values of η at $p_e = 10^3$ Pa (Fig. 7a) and $p_e = 10^6$ Pa (Fig. 7b), respectively. One can see that these coefficients depend strongly on the vibrational level and vary in inverse proportion to the level populations that are less at the upper levels. The comparison of Fig. 7a and 7b shows that the change of the nonequilibrium vibrational distribution significantly influences the self-diffusion coefficients D_{ii}. Figure 8 gives the self-diffusion coefficient of atoms D_{N-N} vs η at different values of p_e, and reports the role of p_e on the D_{N-N} coefficient. D_{N-N} decreases with rising pressure. Such a behavior of the self-diffusion coefficient coincides with the one predicted by the kinetic theory. Thus, in Ref. 15, it is shown that the self-diffusion coefficients grow with the decrease of the number density of corresponding species. The remaining diffusion coefficients are also much less in the case of the high pressure because, in general, all diffusion coefficients are inverse proportional to the total number density.

The data concerning the gas temperature, nonequilibrium level populations and their gradients, the heat conductivity, thermal diffusion, diffusion, and self-diffusion coefficients are used for the calculation of the total heat flux along η at different conditions. Figures 9a and 9b present the total heat flux vs η calculated at $p_e = 10^3$ Pa (Fig. 9a) and $p_e = 10^6$ Pa (Fig. 9b). In Fig. 9a, the roles of the different diffusion processes in the heat transfer are estimated. Thus, curve 1 represents the Fourier part of the heat flux $q_F = -\lambda' \nabla T$ caused by thermal conductivity, curve 2 corresponds to the heat flux calculated when neglecting the diffusion processes, and curve 3 is obtained when neglecting thermal diffusion. It is found that under the conditions considered there exists a strong competition between the diffusion and thermal diffusion processes: just near the surface, thermal diffusion plays a more important role in the heat transfer; the contribution of this process decreases with η from ~100% to 3–5% at the edge. One can notice that thermal diffusion tends to decrease the total heat flux. On the contrary, mass diffusion and diffusion of vibrational energy increase q; the role of the diffusion processes grows from 1% at the wall up to 60–65% at the edge of the boundary layer. Figure 9b gives q and q_F calculated for higher pressure. Under these conditions, the contribution of the thermal diffusion process is negligible (less than 1%) because of the small values of the thermal diffusion coefficients and because the temperature gradient just near the surface is noticeably less than in the previous case. The contribution of the diffusion to the heat transfer is also less in the case of the higher pressure, and reaches 30–35% close to the edge.

The comparison of the total heat flux calculated for different values of pressure is given in Fig. 10. The subscripts 1 and 2 correspond to the low pressure $p_e = 10^3$ Pa and high pressure $p_e = 10^6$ Pa, respectively. This figure shows the effect of the nonequilibrium kinetics on the total heat flux. The high pressure at the edge of the boundary layer corresponds to the conditions that are closer to equilibrium. In this case, the macroscopic parameters in the flow change more slowly, and their gradients are less than in the low-pressure boundary layer. This fact and also the low values of the diffusion coefficients and molar fraction of atoms lead to the weak influence of the diffusion processes on the heat flux, and therefore, $|q_2| < |q_1|$ at $\eta > 1$. On the contrary, the value of q_2 is higher than the value of q_1 at $\eta < 1$, which may be explained by the absence of thermal diffusion tending to decrease the heat flux.

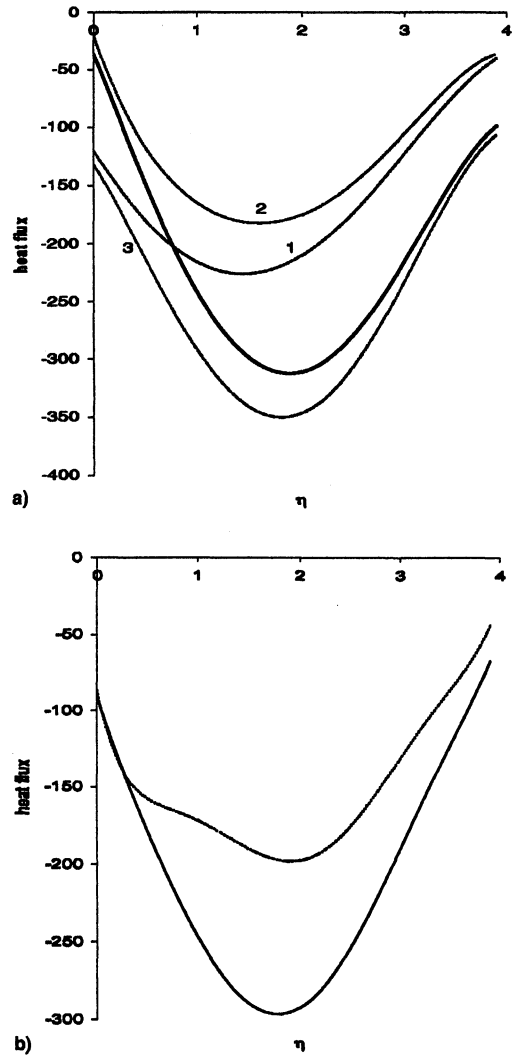

Fig. 9 Heat flux q, in W/m^2, as a function of η at T_e = 5000 K and T_w = 300 K: a) p_e = 10^3 Pa, bold solid curve, total heat flux; curve 1, q_F; curve 2, diffusion is neglected; curve 3, termal diffusion is neglected. b) p_e = 10^6 Pa, solid curve, q; dotted curve, q_F.

The influence of recombination and VV exchange on the heat flux is estimated in Fig. 11. Neglect of these processes leads to an underestimation of the heat flux, particularly near the surface. In this region, recombination and VV exchange provide the higher gradients of the molar fractions of species and level populations. The calculation shows that the Fourier parts of both fluxes are close to one another (the maximum discrepancy of ~15–20% is found just near the surface, then it decreases rapidly with η), and therefore, the difference in the heat flux is mainly caused by the diffusion processes.

The comparison of the total heat flux calculated at different temperature conditions is presented in Fig. 12. One can see that the value of the heat flux computed at higher temperatures, T_e = 7000 K and T_w = 1000 K, is about two times higher than in the case of lower temperatures, particularly in the middle of the boundary layer. It may be pointed out that, in the case T_e = 7000 K, T_w = 1000 K, q practically coincides with q_F (the maximum difference is ~5–6%), and the heat transfer is determined by the temperature gradient.

To estimate the influence of the nonequilibrium vibrational distributions on the heat transfer, the total heat flux is compared with the one calculated on the basis of the equilibrium Boltzmann distribution over vibrational energy with the gas temperature (Fig. 13). The maximum difference reaches 18–20% in the region of strong vibrational nonequilibrium. Approaching the edge of the boundary layer, the vibrational dis-

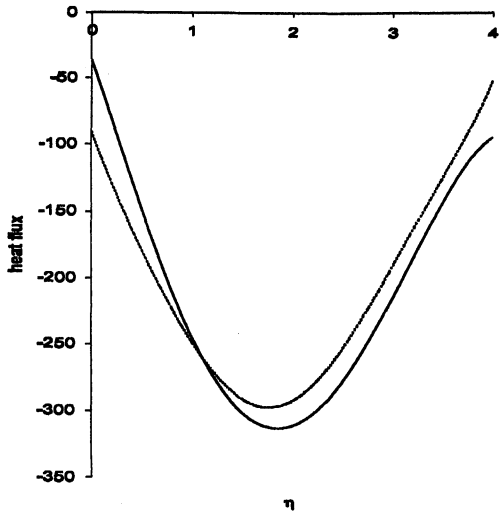

Fig. 10 Total heat flux q, in W/m^2, as a function of η. T_e = 5000 K and T_w = 300 K. Solid curve, q_1, p_e = 10^3 Pa; dotted curve, q_2, p_e = 10^6 Pa.

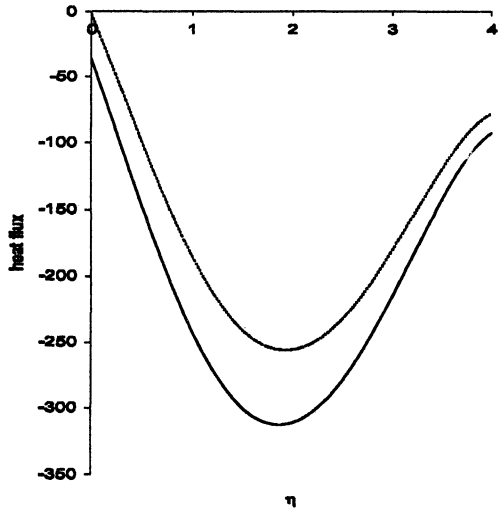

Fig. 11 Total heat flux q, in W/m^2, as a function of η. T_e = 5000 K, T_w = 300 K, and p_e = 10^3 Pa. Solid curve, complete kinetics; dotted curve, no VV exchange and recombination.

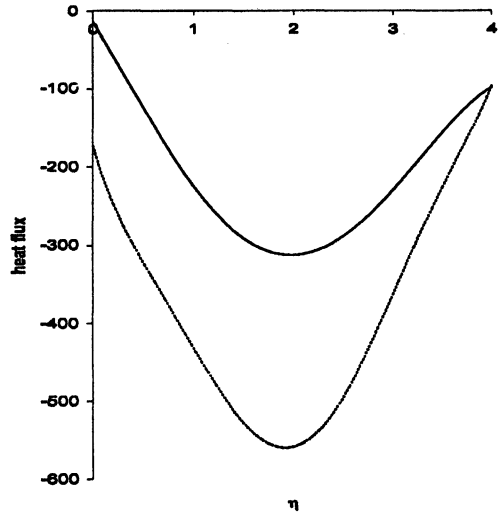

Fig. 12 Total heat flux q, in W/m^2, as a function of η. Solid curve, T_e = 5000 K, T_w = 300 K, p_e = 10^3 Pa; dotted curve, T_e = 7000 K, T_w = 1000 K, p_e = 10^3 Pa.

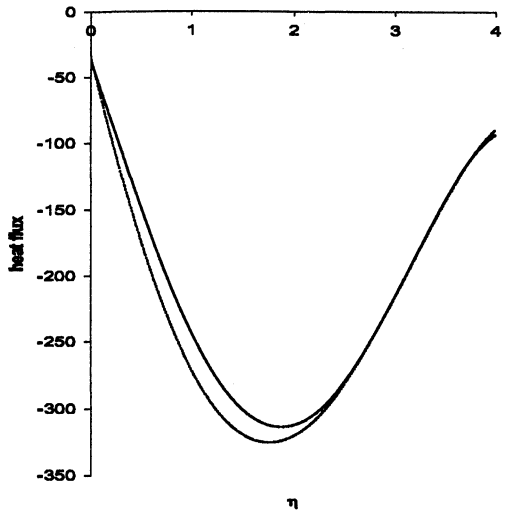

Fig. 13 Total heat flux q, in W/m^2, as a function of η (T_e = 5000 K, T_w = 300 K, p_e = 10^3 Pa). Solid curve, state-to-state approach; dotted curve, Boltzmann distribution.

tributions become close to Boltzmann and the discrepancy between the two fluxes disappears.

Conclusions

In this paper, the transport properties in the boundary layer near the surface of a re-entering body are studied on the basis of the kinetic theory. The heat transfer and diffusion are considered on the basis of the first-order approximation of the generalized Chapman–Enskog method in the state-to-state approach. In this approach, in a mixture of dissociating molecules and recombining atoms, the heat flux and diffusion velocities depend on the gradients of all level populations, atomic number density, and gas temperature. The system of diffusion coefficients contains the coefficients not only for atomic and molecular species, but also for molecules at different vibrational levels. First, the nonequilibrium distributions and gas temperature were examined along the streamline orthogonal to the surface; then the heat flux, heat conductivity, and all diffusion coefficients were computed using these data for the same conditions. The results show the influence of nonequilibrium kinetics on the heat transfer and diffusion.

Recombination–dissociation processes affect the level populations and transport properties of the flow. Dissociation near the high-temperature edge of the boundary layer produces atoms that diffuse toward the cool surface; recombination near the wall pumps the vibrational levels and leads to the strong nonequilibrium vibrational distribution. The effect of the nonequilibrium kinetics on the gas temperature, heat conductivity coefficient, and total heat flux is not so strong as on the level populations; however, it noticeably changes the behavior of the gas temperature and heat flux: recombination near the wall leads to an increase in T and q.

To estimate the influence of the nonequilibrium level populations on the transport properties, two values of the pressure at the edge of the boundary layer were considered. The increase of the pressure gives the vibrational distributions that are closer to the equilibrium; it leads to the lower value of the heat flux. The heat conductivity and all diffusion and thermal diffusion coefficients depend strongly on the pressure p_e. The transport of vibrational energy by excited molecules gives a contribution to the heat transfer near the surface, which is comparable with the contribution of the mass transfer caused by the diffusion of chemical species. Under the high-pressure conditions, the effect of thermal diffusion on the heat flux is weak and may be neglected, whereas the neglect of this process under the strong nonequilibrium conditions leads to a significant overestimation of the heat flux close to the surface. The role of the diffusion processes becomes more important toward the edge of the boundary layer, and decreases at high p_e and T_e. With T_e rising (T_e = 7000 K), the contribution of all diffusion processes to the total heat flux occurs weakly due to the high degree of dissociation, and the gas temperature gradient plays the most important role in the heat transfer in the boundary layer.

In conclusion, it may be pointed out that this study was performed inserting the nonequilibrium kinetics obtained on the basis of simplified Eqs. (15) and (16) into the transport theory algorithm. This model permits one to investigate the influence of the nonequilibrium distributions on transport properties. To estimate the inverse influence of diffusion of excited molecules on the level populations, one should use the more rigorous Eqs. (1–4), which follow from the kinetic equations and describe simultaneously the nonequilibrium kinetics and transport properties of the flow in the state-to-state approach.

Acknowledgment

This work has been partially supported by Agenzia Spaziale Italiana. E. Nagnibeda thanks CNR for the grant.

References

[1]Shizgal, B., and Lordet., F., "Vibrational Nonequilibrium in a Supersonic Expansion with Reactions: Application to O_2 – O," *Journal of Chemical Physics*, Vol. 104, No. 10, 1996, pp. 3579–3597.

[2]Kustova, E. V., and Nagnibeda, E. A., "The Effect of Level Nonequilibrium Kinetics on Transport Properties of Dissociating Gas Flow Behind a Shock Wave," *Proceedings of the 21st International Symposium on Shock Waves* (Brisbane, Australia), edited by A. F. P. Houwing, Univ. of Queensland, Queensland, Australia, 1997 (Paper 4231).

[3]Varghese, P. L., and Gonzales, D. A., "Nonequilibrium Chemistry Models for Shock-Heated Gases," edited by M. Capitelli, *Molecular Physics and Hypersonic Flows*, Kluwer, Dordrecht, The Netherlands, 1996.

[4]Meolans, J. G., Mouti, M., Lordet, F., and Chauvin, A. H., "Vibration-Dissociation Coupling Behind a Plane Shock Wave," *Rarefied Gas Dynamics 19*, edited by J. Harvey and G. Lord, Vol. 1, Oxford Univ. Press, Oxford, England, UK, 1995.

[5]Capitelli, M., Armenise, I., and Gorse, C., "State-to-State Approach in the Kinetics of Air Components Under Re-Entry Conditions," *Journal of Thermophysics and Heat Transfer*, Vol. 11, No. 4, 1997, pp. 570–578.

[6]Belouaggadia, N., and Brun, R., "Chemical Rate Constants in Nonequilibrium Flows," AIAA Paper 97-2555, June 1997.

[7]Armenise, I., Capitelli, M., and Gorse, C., "Fundamental Aspects of the Coupling of Nonequilibrium Vibrational Kinetics and Dissociation-Recombination Processes with the Boundary Layer Fluid Dynamics in N_2 and Air Hypersonic Flows," *NATO ASI Molecular Physics and Hypersonic Flows*, Vol. 482, Series C: Mathematical and Physical Sciences, Kluwer, Dordrecht, The Netherlands, 1996.

[8]Candler, G. V., Olejniczak, J., and Harrold, B., "Detailed Simulation of Nitrogen Dissociation in Stagnation Regions," *Physics of Fluids*, Vol. 9, No. 7, 1997, pp. 2108–2117.

[9]Ludwig, G., and Heil, M., "Boundary Layer Theory with Dissociation and Ionization," *Advances in Applied Mechanics*, Vol. 6, Academic, New York, 1960.

[10]Brun, R., "Transport Properties in Reactive Gas Flows," AIAA Paper 88-2655, June 1988.

[11]Kustova, E. V., and Nagnibeda, E. A., "The Influence of Non-Boltzmann Vibrational Distribution on Thermal Conductivity and Viscosity," *Molecular Physics and Hypersonic Flows*, edited by M. Capitelli, Kluwer, Dordrecht, The Netherlands, 1996.

[12]Doroshenko, V. M., Kudryavtsev, N. N., Novikov, S. S., and Smetanin, V. V., "Influence of the Formation of Vibrationally Excited Molecules in Gas Phase Recombination on the Surface Heat Flux," *High Temperature*, Vol. 28, 1990, pp. 82–89.

[13]Kustova, E. V., and Nagnibeda, E. A., "Transport Properties of a Reacting Gas Mixture with Strong Vibrational and Chemical Nonequilibrium," *Chemical Physics*, Vol. 233, 1998, pp. 57–75.

[14]Chikhaoui, A., Dudon, J. P., Kustova, E. V., and Nagnibeda, E. A., "Transport Properties in Reacting Mixture of Polyatomic Gases,"

Journal of Physica A, Vol. 247, Nos. 1–4, 1997, pp. 526–552.

[15]Ferziger, J. H., and Kaper, H. G., *Mathematical Theory of Transport Processes in Gases*, North-Holland, Amsterdam, 1972.

[16]Hirschfelder, J. O., Curtiss, C. F., and Bird, R. B., *The Molecular Theory of Gases and Liquids*, Wiley, New York, 1954.

[17]Capitelli, M., Celiberto, R., Gorse, C., and Giordano, D., "Transport Properties of High Temperature Air Components: A Review," *Plasma Chemistry and Plasma Processing*, Vol. 16, No. 1, 1996, pp. 2678–3028 (Supplement).

[18]Armenise, I., Capitelli, M., and Gorse, C., "On the Coupling of Non-Equilibrium Vibrational Kinetics and Dissociation–Recombination Processes in the Boundary Layer Surrounding a Hypersonic Reentry Vehicle," *Aerothermodynamics for Space Vehicles*, edited by J. J. Hunt, ESTEC, ESA Publication Div., Noordwijk, The Netherlands, 1995.

[19]Billing, G. D., and Fisher, E. R., "VV and VT Rate Coefficients in N_2 by a Quantum-Classical Model," *Chemical Physics*, Vol. 43, 1979, pp. 395–401.

[20]Lagana, A., and Garcia, E., "Temperature Dependence of N + N_2 Rate Coefficients," *Journal of Chemical Physics*, Vol. 98, 1994, pp. 502–507.

[21]Vargaftick, N. B., *Handbook of Physical Properties of Liquids and Gases—Pure Substances and Mixtures*, 2nd ed., Hemisphere, New York, 1975.

[22]Thomson, R. M., "The Thermal Conductivity of Gases with Vibrational Internal Energy," *Journal Physics D: Applied Physics*, Vol. 11, 1978, pp. 2509–2546.